ELSEVIER

Thermochimica Acta 389 (2002) 141–151

thermochimica acta

www.elsevier.com/locate/tca

The thermal analysis of nonezymatic glycosylation of human serum albumin: differential scanning calorimetry and circular dichroism studies

A. Mohamadi-Nejad[a,b], A.A. Moosavi-Movahedi[a,*], S. Safarian[a], M.H. Naderi-Manesh[c], B. Ranjbar[c], B. Farzami[d], H. Mostafavi[e], M.B. Larijani[f], G.H. Hakimelahi[g]

[a]*Institute of Biochemistry & Biophysics, University of Tehran, P.O. Box 13145-1384, Tehran, Iran*
[b]*Faculty of Premedical Sciences, Medical Sciences University of Mashhad, Mashhad, Iran*
[c]*Department of Biophysics, Faculty of Sciences, Tarbiat Modares University, Tehran, Iran*
[d]*Department of Biochemistry, Medical Sciences University of Tehran, Tehran, Iran*
[e]*The National Research Center for Genetic Engineering and Biotechnology, Tehran, Iran*
[f]*The Research Center of Diabetes, Dr. A. Shariati Hospital, Tehran, Iran*
[g]*Institute of Chemistry, Academia Sinica, Taipei, Taiwan, ROC*

Received 28 August 2001; received in revised form 14 December 2001; accepted 3 January 2002

Abstract

The stability of human serum albumin (HSA) is studied before and after incubation with glucose utilizing differential scanning Calorimetry (DSC) and circular dichroism (CD) techniques. The incubation of HSA with glucose results in its nonenzymatic glycosylation that is glycosylated HSA (GHSA) formed in glucose concentrations (8.25, 16.5 and 27.5 mM) in a temperature dependent manner. The DSC profiles of GHSA samples, which indicate changes in heat capacity C_p and C_p^{excess} versus temperature, were obtained and the thermal denaturation reversibility of each sample was assessed up to 80 °C. The melting point (T_m), the change of enthalpy, and the heat capacity for GHSA at different glucose concentrations were obtained. The results showed that glucose at lower concentrations induces the destabilization of HSA while at higher concentrations induces its stabilization. In addition, considerable conformational changes in HSA were observed after incubation with glucose. This was demonstrated through deconvolution of DSC profiles that imply the formation of new energetic domains, which were further confirmed by the presence of α-helices in the CD spectrum.

Keywords: HSA; Glycosylation; Thermal analysis; DSC; CD

1. Introduction

Human serum albumin (HSA) is a single chain polypeptide of 585 residues, which comprises about 60% of the plasma protein. It is the major contributor to the oncotic pressure of blood [1]. In addition, it has been reported that albumin is chiefly responsible for the maintenance of blood pH [2,3]. In human, the albumin is synthesized by the liver [4] and posses a half-life in circulation of 19–20 days [5,6]. The HSA is named a multifunctional plasma carrier protein because of its ability to bind to an unusually broad

* Corresponding author. Tel.: +98-21-640-3957; fax: +98-21-640-4680.
E-mail address: moosavi@ibb.ut.ac.ir (A.A. Moosavi-Movahedi).

0040-6031/02/$ – see front matter
PII: S0040-6031(02)00006-0

spectrum of ligands. These include inorganic cations, organic anions, various drugs, amino acids, and perhaps most important and physiologically available hydrophobic molecules such as bilirubin and fatty acids [1,7,8].

There is a large body of evidence that under physiological conditions, glucose reacts nonenzymatically with a wide variety of proteins to form Schiff bases which then transform to Amadori products that are relatively stable [9–13]. The nonenzymatic glycosylation of HSA has been demonstrated to alter its conformation and function [1,14].

The interaction between HSA and glucose has been studied utilizing a variety of techniques. The study of conformational and functional changes of HSA after interaction with glucose by fluorescence techniques showed two phenomena. The first is the reduction of fluorescence intensity and the second is a shift in λ at maximum intensity of emission toward lower wavelength. This implies that conformational changes have occurred. Alterations in the binding affinity of HSA for some ligands before and after interaction with glucose indicates functional changes due to glycosylation [1].

Determination of the glucose exclusive binding sites on HSA was studied precisely via boronic acid affinity chromatography and amino acid analysis techniques [15]. In this study, it was declared that Lys 525 is the more preferential site for glucose binding to HSA when compared to other lysine residues (there are 60 lysine residues in HSA). Another site that becomes glycosylated on HSA is Lys 199. Its ϵ-amino group has a pK_a of about 8–8.7, whereas the other lysines' ϵ-amino group are likely to have a pK_a value near 11. The lower pK_a should favor the reaction of the amino group with glucose, and in each case the reactive amino group must be uncharged in order for glycosylation to occur [15]. Therefore, other lysine residues do not participate in chemical modifications.

Early studies have shown that nonenzymatic glycosylation occurs only at ϵ-amino groups of lysine residue in serum albumin [16,17]. In addition, some percentage of human albumin in serum is naturally in a glycosylated form. Depending on the technique utilized, this percentage varies, i.e. 6–15 [18] or 10–12% [15] were reported by chromatography, 8–16% by Thiobarbituric acid (TBA) assay [19], 28% by HPLC methods [20], and 29% by radiolabled technique [21].

The interaction of some ligands with HSA and GHSA have also been examined. The aspirin binding to HSA varied when compared to GHSA. A reduction in the binding affinity to GHSA was observed [18]. Interaction of bilirubin and long chain fatty acids are also affected after nonenzymatic glycosylation of HSA. The affinity of binding (K) decreases significantly, for example equilibrium constant of binding (K) for fatty acid to HSA is 20-fold of the binding to GHSA [17,18]. Similar results were obtained for salicylate binding [22].

Incubation of glucose with HSA in solution for a long period of time (at least 10 days) causes another phenomenon, namely over-glycosylation. The glycosylated lysine residues of two neighboring chains of HSA interact with each other in an irreversible manner. This product is stable and is known as advanced glycation end product (AGE), which relates to the diabetes complications [23,24]. This effect causes crosslinking of GHSA, hence, influencing its normal functions. The AGE effect is one of the major causes of the chronic illness and high mortality associated with diabetes [25,26].

Almost all of the studies described above lack a thermodynamic point of view of glucose interaction with HSA. The main goal of the studies described here is to determine the thermodynamic changes that are associated with glycosylation of HSA and the interpretation of its conformational changes.

2. Materials and methods

β-D(+)-Glucose was analytical grade and purchased from Sigma. Membrane filters with 0.2 μm pore size and 25 mm in diameter were purchased from Whatmann (UK). All of the other materials were of analytical grade and purchased from Merck (Germany). All solutions were prepared with double distilled water.

2.1. HSA preparation

Cohn albumin fraction V was prepared from normal adults serum and was further purified by preparative HPLC (Beckman, reverse phase, C4 column: 21 mm × 250 mm, pump model 125, UV-detector model 168, USA). The preparation showed 97.3259% purity of monomeric form when tested by analytical HPLC

(Knauer type 6400, Tosohaas SK gel-3000, Japan) and electrophoresis (Ciba Corning-710, Germany) (data is not shown). The experiment was tested to compare our prepared fraction V with sample fraction V from Sigma. The results were markedly consistent with Sigma fraction V (data is not shown). Since our goal was the study of nonenzymatic glycosylation of HSA at physiological conditions therefore we chose the albumin fraction V. Analytical reversed phase HPLC was performed on a Vydac C4 column (5 u, 300 Å, 4.6 mm × 250 mm; buffer A: 0.1% triflouroacetic acid (TFA) in water, buffer B: 0.1% TFA, acetonitrile/water 4:1 v/v, flowrate: 0.8 ml/min, detection at 215 nm, gradient: 0–100% B in 30 min, injection volume: 20 μl; concentration: 1 mg/ml, retention time: 24.7 min). Preparative purification of Cohn albumin fraction V was carried out on a Vydac C4 column (21 mm × 250 mm; flow rate: 8 ml/min) with the same method.

An amount of 2 ml of stock protein solution was dialysed against sodium phosphate buffer 2.5 mM, pH 7.4 at 4 °C for 72 h. The protein concentration was determined spectrophotometrically (by UV-3100, Shimadzu, Japan), using $\varepsilon^{1\%} = 5.3$ at 280 nm [12].

Under sterile conditions, four separate samples of protein solution at concentration of 0.6 mM (40 mg/ml) were prepared (in 2.5 mM phosphate buffer, pH 7.4). In four cleaned glass tubes, three of which containing glucose at following concentrations: 8.25, 16.5 and 27.5 mM and one with no glucose. The samples were incubated at 37 °C for 1 week, and then prepared for differential scanning calorimeter (DSC) and circular dichroism (CD) studies. The protein concentrations utilized for DSC and CD were at 2 and 0.15 mg/ml, respectively.

DSC experiments with 0.328 ml cells were carried out in a computer-matched Scal-1 (Russian Academy of Science, Pushchino, including Scanscal, Wscal, Scal-2 software programs). Circular dichroism experiments were carried out in a computer-matched Jasco-J715 Spectropolarimeter (Japan) in the range of 185–250 nm at 310 K that includes a thermal unit. Thermally induced unfolding was assayed at 222 nm in the range of 25–90 °C. The molar ellipticity was determined as

$$[\theta]_\lambda = \frac{\theta_\lambda \times \mathrm{MRW}}{c \times l}$$

where c is protein concentration in mg/ml and l is the length of the light path in the cell, θ_λ is the measured ellipticity in degrees at wavelength λ, MRW is the averaged molecular weight of an amino acid residue, taken as 116.4 [27].

2.2. Thermal denaturation

Thermal induction of unfolding was assayed by DSC technique. Calibration of the instrument was carried out automatically using Wscal software through the input calibration pulse of 25 μW. In this manner, the calculated sensitivity for the instrument was equal to 21.53 nW/unit.

Determination of the linear dependence of temperature on the signal magnitude was performed in the temperature range of 25–85 °C using Scanscal program. The calculated parameters was saved and used as a calibration file during the thermal scanning.

The measuring heat capacity of protein samples (C_p) versus temperature (T) as described previously by Privalov and Potekhin [28]. The scan rate was 1 K/min at a constant pressure of 2 atm over the liquids in the cells. The heat capacity difference of the cells (in which one of the cells is loaded with protein solution to be studied and the other with solvent, containing all the constituents of the sample solution except for the protein, i.e. buffer + glucose as the reference solvent) was measured by the compensation method: the controller automatically monitors the power in the electric heaters of both cells to maintain identity of their temperatures at heating, and the difference of these powers is recorded as a temperature function [28]. The differential electrical power between the two cells was normalized using the scanning and the electrical calibration of the calorimeter to obtain a curve of the relative heat capacity (C_p) versus temperature (T). The calorimetric data were corrected according to Sturtevant equations to obtain finally the excess heat capacity profiles for calculation of the differences in heat capacity between the initial and the final state and the melting enthalpies [29–32].

The thermodynamic parameters were obtained as described in [27,28,33–39]. The total change of enthalpy of the system can be obtained by measuring the area under thermogram (C_p versus T profile) $\left(\Delta H_{\mathrm{total}} = \int_{T_\mathrm{i}}^{T_\mathrm{f}} C_p \, \mathrm{d}t\right)$ where T_i and T_f are the initial and final temperatures that, contain the change of

enthalpy of native $\left(\int_{T_i}^{T} C_p^N \, dT\right)$ and denatured $\left(\int_{T}^{T_f} C_p \, dT\right)$ form and transition phenomena at temperature T (ΔH_D) therefore, for every temperature (T) we can write

$$\Delta H = \int_{T_i}^{T_f} C_p \, dT \tag{1}$$

or

$$\Delta H_{total} = \Delta H_D(T) + \int_{T_i}^{T} C_p^N \, dT + \int_{T}^{T_f} C_p^D \, dT \tag{2}$$

where C_p^N, C_p^D are the heat capacities of protein at native and denatured state respectively, if we rearrange Eq. (1) for T_m then we will have

$$\Delta H_{total} = \Delta H(T_m) + \int_{T_i}^{T_m} C_p^N \, dT + \int_{T_m}^{T_f} C_p^D \, dT \tag{3}$$

where $\Delta H(T_m)$ is the change of enthalpy due to denaturation of protein at melting point (T_m). By ordering the Eq. (2) and combining it with Eq. (3), we can obtain

$$\Delta H(T) = \Delta H(T_m) - \int_{T}^{T_m} \Delta C_p \, dT \tag{4}$$

where

$$\Delta C_p = C_p^D - C_p^N \tag{5}$$

is the slope of $\Delta H(T)$ diagram.

3. Results

3.1. DSC results

Figs. 1–3 show the variation of C_p^{excess} of HSA versus temperatures when incubated with different concentrations of glucose, 8.25, 16.5 and 27.5 mM, respectively. The reversibility of thermal denaturation of the samples up to 80 °C was assayed by rescanning after cooling the sample that was previously scanned thermally. Also, they contain the deconvolution results of thermal profile (deconvolution of excess heat capacity into sequential two-state transitions was carried out in upward direction (from low to high temperature) by utilization of Scal-2 software. The resulting deconvolution parameters were optimized by the fitting program of the related software. The calculated fitting error for all of the samples was less than 0.015) that present energetic domains with special T_m and enthalpy of unfolding (ΔH_m) as shown in Table 1. The thermal denaturation profile of HSA in the absence of glucose was reversible up to 75 °C but irreversible above 75 °C (data was not shown). Therefore, the denatured line was not accessible and it is impossible to obtain the deconvolution profile for HSA in the absence of glucose. It is important to note it was previously reported in literature regarding HSA alone, this process did not allow to obtain the C_p values of the unfolded state, therefore the thermogram was obtained by heating the protein up to 74 °C and the C_p values of the denatured form was obtained by simulation using non-linear regression fitting of data [31,32].

Figs. 1–3 show thermogram of C_p^{excess} versus temperature for HSA in the presence of glucose at different concentrations. Fig. 1 demonstrates a small shoulder (320–325 K) for initiation of compactness in a part of the protein in the presence of 8.25 mM (150 mg/dl) glucose. Fig. 2 shows two main peaks that imply two distinct parts for HSA in the presence of 16.5 mM (300 mg/dl) glucose, which unfold separately. After deconvolution, it reveals five energetic

Table 1
Data information for human serum albumin after interacting with glucose at concentrations such as: 1.5 mg/ml (8.25 mM, including D1–D3), 3 mg/ml (16.5 mM, including E1–E5) and 5 mg/ml (27.5 mM, including F1–F4) at 2.5 mM phosphate buffer, pH 7.4 at 37 °C for 1 week

Domains	ΔH (kJ/mol)	T_m (K)	ΔC_p (kJ/mol K)
D1	254.2	326.5	–
D2	431.8	334.2	–
D3	395.9	338.5	–
Total	1081.9	335.68	88.4
E1	212.4	302.4	–
E2	226.9	312.4	–
E3	186.6	325.9	–
E4	424.3	334.5	–
E5	336	339.3	–
Total	1386.2	335.38	83
F1	240.7	306.4	–
F2	275.4	316.2	–
F3	277.9	325	–
F4	452.6	334.7	–
Total	1246.7	334.5	39

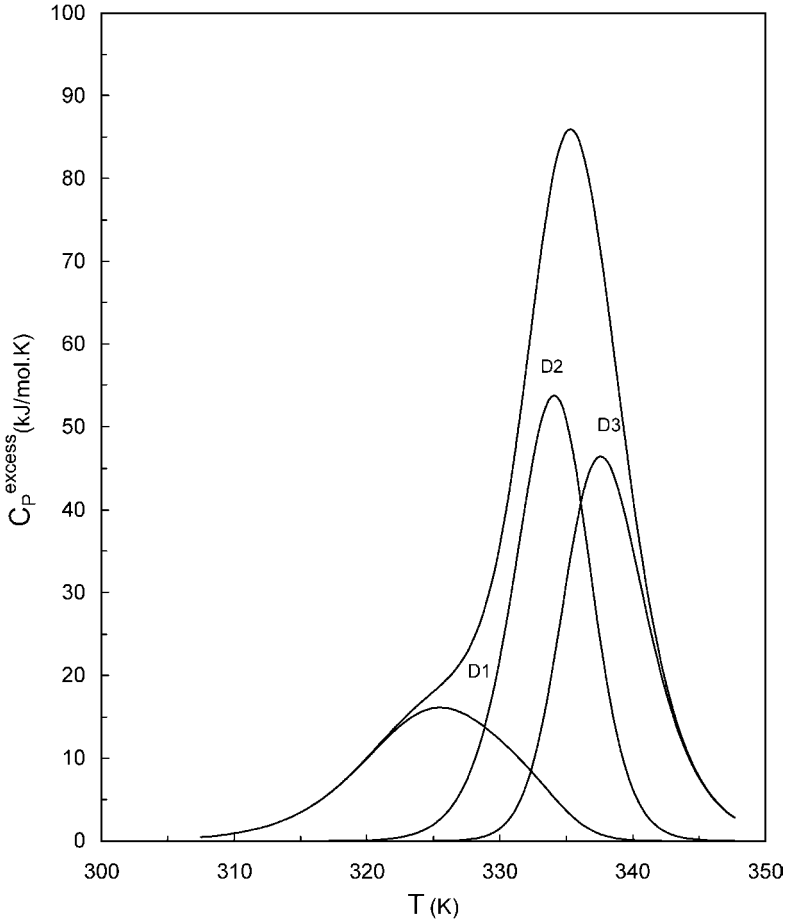

Fig. 1. Thermogram of human serum albumin (HSA) in the presence of 8.25 mM glucose and is incubated at 37 °C, in 2.5 mM phosphate buffer for 1 week. Subpeaks (D1–D3) were obtained by deconvolution of C_p^{excess} profile.

domains (subpeaks E1–E5). In this case, the denaturation of glycosylated human serum albumin (GHSA) occurred with five states and the melting point (T_m) and the enthalpy of melting of each domain (ΔH_m) were obtained and shown in Table 1.

Fig. 3 also shows two distinct peaks for HSA in the presence of 27.5 mM (500 mg/dl) glucose. This implies that the denaturation of each part occurred at different temperatures among the four energetic domains (subpeaks, F1–F4) with value of T_m and ΔH_m (see Table 1).

3.2. CD results

The far-UV CD spectra of HSA in the absence and the presence of different glucose concentrations are presented in Figs. 4 and 5. As evident, the spectra are typical for α-helices with two minima at about 208 and 222 nm. According to Fig. 4, in the presence of 8.25 mM glucose, (Fig. 4a) the content of α-helices decreased, but treatment with a higher concentrations of the glucose 16.5 mM (Fig. 4d) led to an increase in the extent of secondary structure. However, treatment with 27.5 mM glucose (Fig. 4c) led to a decrease in the content of α-helices in comparison with 16.5 mM and increase relative to alone HSA (Fig. 4b). To collate the thermodynamic and structural data, we took the melting curves for HSA in the absence or presence of different glucose concentrations, i.e. the CD versus temperature in the far-UV (222 nm) (Fig. 5).

Fig. 4 shows the far-UV CD spectra of HSA in the range of 185–250 nm in the absence or presence of different glucose concentrations (8.25, 16.5 and

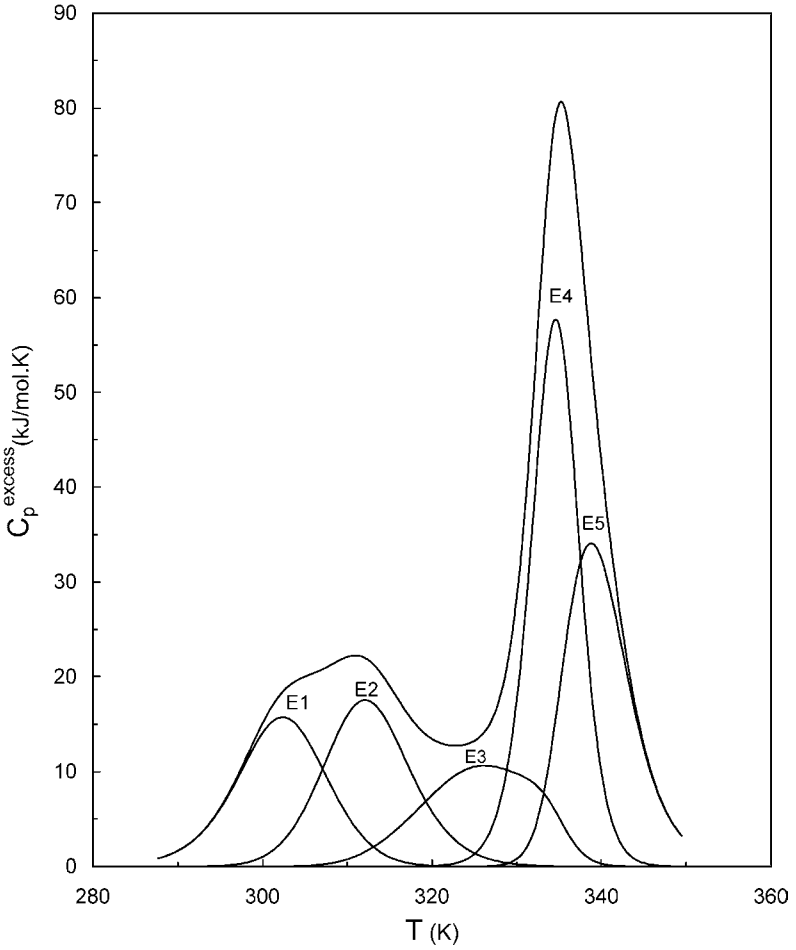

Fig. 2. Thermogram of human serum albumin (HSA) in the presence of 16.5 mM glucose and is incubated at 37 °C, in 2.5 mM phosphate buffer for 1 week. Subpeaks (E1–E5) were obtained by deconvolution of C_p^{excess} profile.

27.5 mM), at 37 °C. The results were expressed as molar ellipticity, $[\theta]_\lambda$ (degree cm^2 dmol^{-1}), based on the average amino acid residue molecular weight (MRW). Therefore, the sample with 16.5 mM glucose has more secondary structure (α-helices) than other samples.

Fig. 5 shows the variation of molar ellipticity of the cited four samples versus temperature in the range of 25–90 °C. The CD thermal profiles, including 16.5 mM glucose (Fig. 5d), showed a higher right hand shift relative to other glucose concentrations indicating that the protein is more stable under this condition relative to other conditions. Thus, the higher stability of HSA in the presence of 16.5 mM glucose corresponds with an increase in α-helices in the secondary structure, which correlates with DSC results (E3, Fig. 2).

4. Discussion

The human serum albumin was incubated with different concentrations of glucose, 8.25 mM (150 mg/dl, the condition of initiation of diabetes mellitus), 16.5 mM (300 mg/dl, the condition of general diabetes mellitus) and 27.5 mM (500 mg/dl, the condition of acute diabetes mellitus). It is evident that as the glucose concentration increases the binding of glucose to HSA is enhanced, that is more amount of HSA is glycosylated.

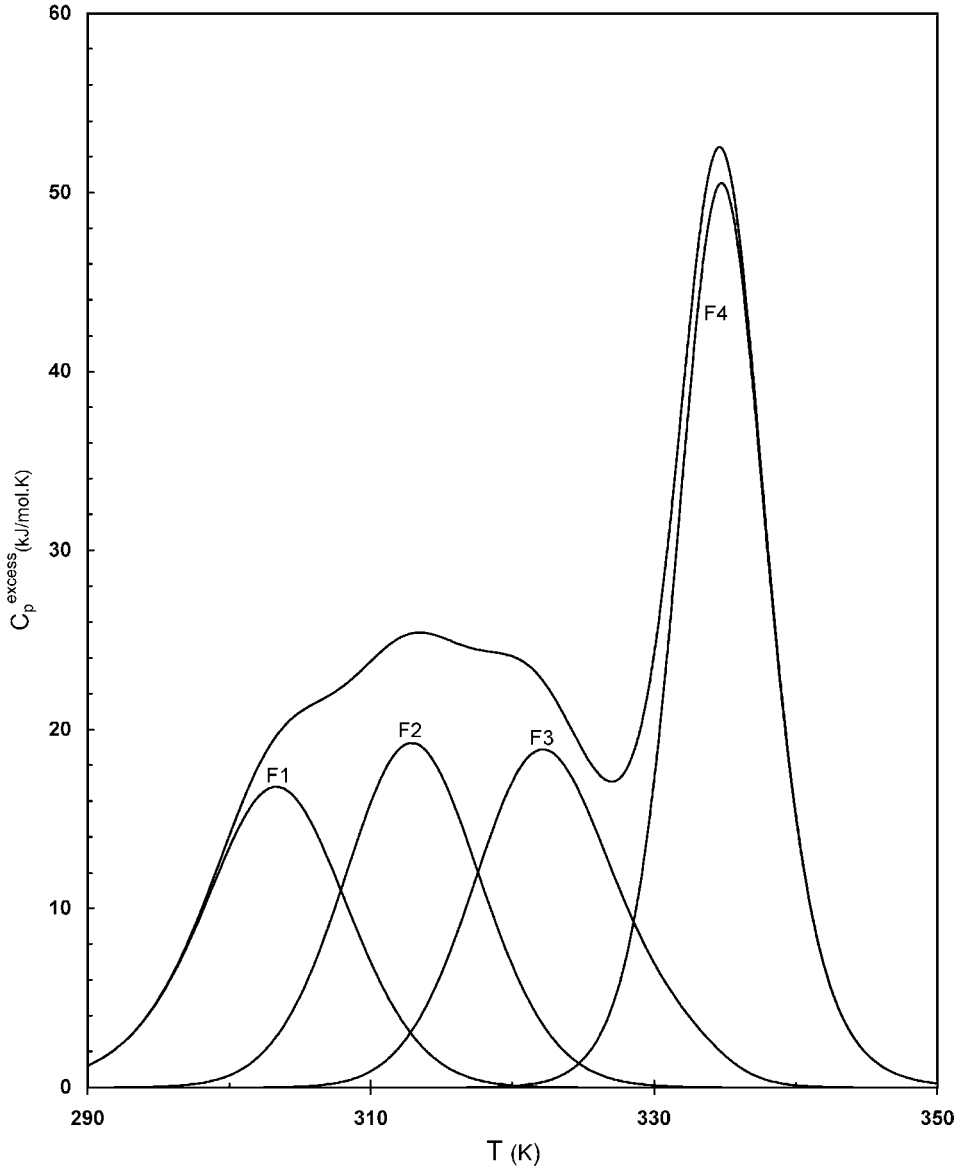

Fig. 3. Thermogram of human serum albumin (HSA) in presence of 27.5 mM glucose and is incubated at 37 °C, in 2.5 mM phosphate buffer for 1 week. Subpeaks (F1–F4) were obtained by deconvolution of C_p^{excess} profile.

HSA, has three nearly equal domains (conventionally referred to as I, II and III). Furthermore, each domain is divided into two near symmetrical subdomains named A and B [40,41]. The X-ray crystallographic data and the three-dimensional structure of HSA showed two distinct segments. One extra compacted segment as the head of HSA molecule, which is the result of intermolecular interactions of IA, IB and IIA subdomains. Whereas another segment, the tail of the molecule, is more extended than the head part and contains IIB, IIIA and IIIB subdomains. The stability of the tail is less than the head part and has a loose conformation when compared to the head region [40,41] (see Figs. 2 and 3 from references [40,41], respectively). The Trp 214 is conserved in mammalian albumins and plays an important structural role in the

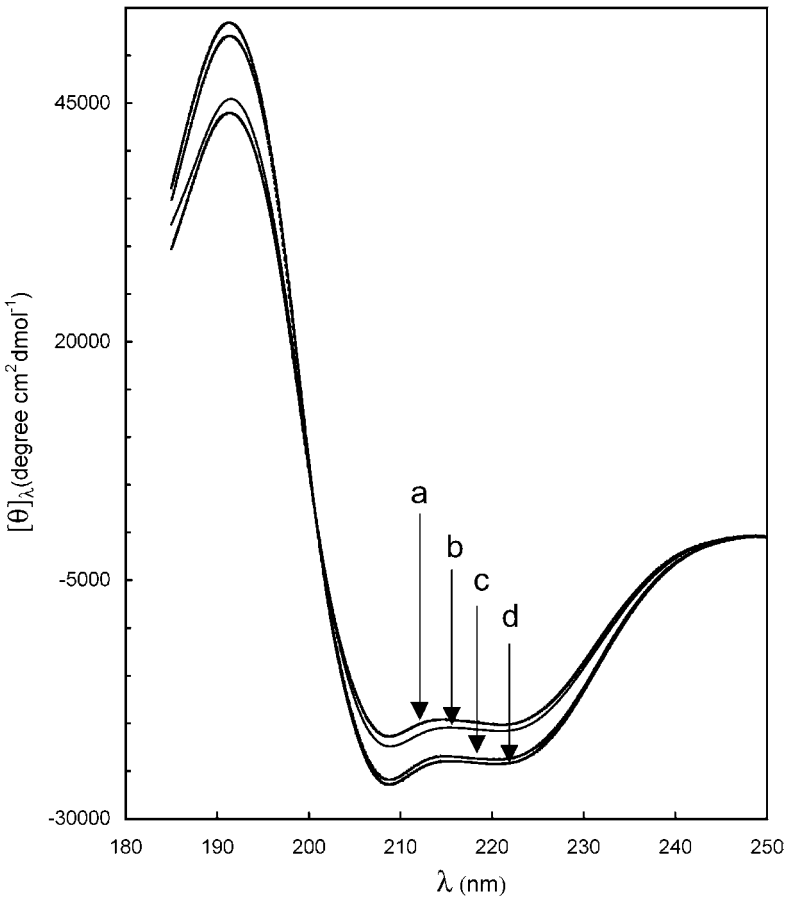

Fig. 4. The molar elipticity of human serum albumin (HSA) vs. wavelenghts, (a) 8.25 mM glucose, (b) in the absence of glucose, (c) 27.5 mM glucose, and (d) 16.5 mM glucose and in 2.5 mM phosphate buffer, pH 7.4 at 37 °C after 1 week incubation.

formation of the IIA binding site by limiting the solvent accessibility. In addition, it participates in additional hydrophobic packing interactions between IIA and IIIA interface. This is the reason that HSA takes the heart shape [41]. The complete X-ray conformational structure, including the six subdomains, is demonstrated in [40,41].

The studies of energetic domains (D, E and F) of GHSA with more detail were performed by DSC and CD techniques. The deconvoluted profile of DSC for GHSA (8.25 mM) showed three energetic domains (Fig. 1). The interaction of glucose with HSA compacts some part of the structure. Glucose interacts with Lys 525 at first (placed in IIIB) imposing the shoulder (around 324 K). This demonstrates a decrease in interaction of IIIB with its neighboring subdomains. There is higher thermal stability for subdomains of A relative to subdomains of B. This is due to each subdomain of A having two more s–s bonds as well as more α-helices relative to each subdomain of B. On the other hand, subdomains of IB and IIB fenced by IA and IIA, and IIA and IIIA, respectively [40,41] (see Figs. 2 and 3 from [40,41], respectively). Therefore, the subdomain of IIIB having more freedom related to subdomain of IIB and unfolds thermally first, hence, the subpeak of D1 is related to IIIB. In addition, there are six almost equal subdomains for HSA and the ΔH_m for D1 (254 kJ/mol) shows a value of near to one-sixth of total ΔH of denaturation (1082 kJ/mol). Precision of T_m and melting enthalpy values which have been determined for each thermal profile was confirmed through the double repeating of the experiment with the new injection of the sample and reference solutions into the related cells of the instrument.

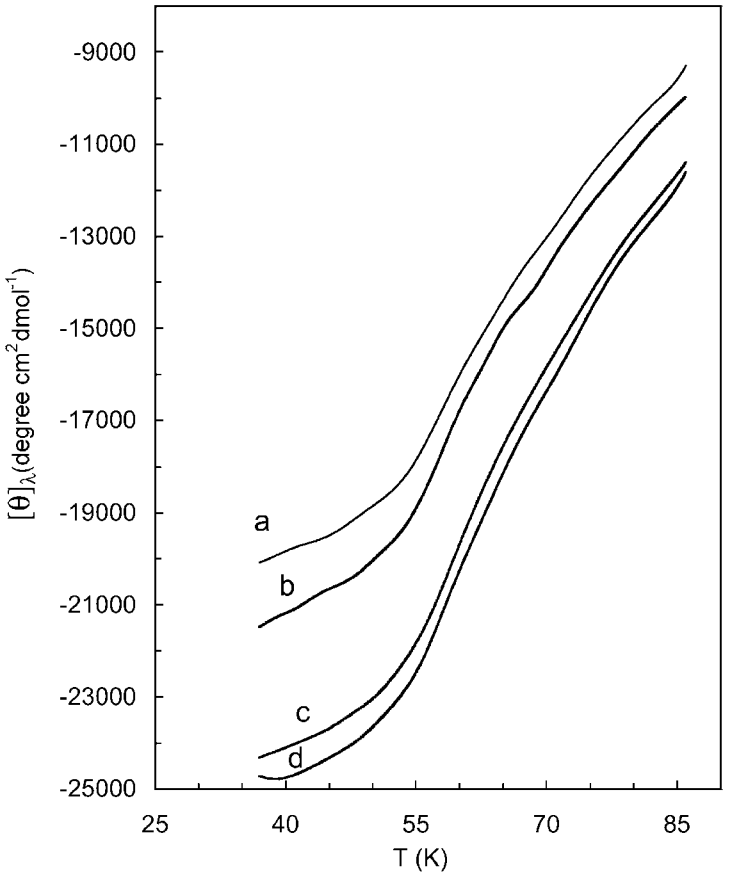

Fig. 5. The molar elipticity of human serum albumin (HSA) vs. temperatures, at wavelength of 222 nm, (a) 8.25 mM glucose, (b) in the absence of glucose, (c) 27.5 mM glucose, and (d) 16.5 mM glucose in 2.5 mM phosphate buffer, pH 7.4 at 37 °C after 1 week incubation.

The values of enthalpy and T_m for D3 (Fig. 1) are equal to 395 kJ/mol and 338.5 K, respectively. The D3 corresponds to subdomains IIA and IIIA. The IIA and IIIA subdomains have powerful hydrophobic interactions between their interface [41] contributing to the higher stabilization of their structure (higher T_m). The subpeak of D2 belongs to IA, IB and IIB. However, IIB is restricted by III and IA via their powerful hydrophobic interactions, and IA and IB are placed at compacted head region. Therefore, the thermal unfolding of D2 must be higher than D1, but less than D3.

When glucose concentration is increased to 16.5 mM, the corrected DSC profile demonstrated two distinct physical peaks, or its C_p^{excess} profile has two phases (Fig. 2). Thus, the thermal denaturation of different segments of GHSA under this condition occurs at two distinct phases with less co-operativity between them (compared to Fig. 1) [32]. The first peak is connected to a certain rearrangement, as a result of which it becomes more compact and its capacity for intramolecular interaction changes [35]. This important observation was also noted with CD technique. As evident, temperature dependencies of the CD elipticity was not sigmoidal (S-shape) which is not a characteristic of cooperative ''all-or-none'' melting process. This confirms with the calorimetric results and shows that the hydrophobic interactions between the tail (via IIIA) and the head (via IIA) of HSA were decreased after incubation with glucose. This is perhaps due to the ability of glucose to compact the subdomains via binding to HSA and/or alterations in physical properties of the surroundings. Therefore, the thermal denaturation of the tail and the head parts of GHSA molecule appear more distinctly. The result

of interaction of the glucose with HSA is the compactness of the subdomains that take part in these interactions. Thus, after glycosylation of HSA intersubdomains interactions were reduced. This is the reason for reduction in co-operativity between the head and the tail parts in thermal denaturation and also a more clear distinction between energetic domains were observed. The deconvolution of C_p^{excess} profile of GHSA (16.5 mM) introduces two energetic domains at the tail part, two energetic domains at the head part and one small subpeak (E3) that is common between the two parts (Fig. 2). The latter suggests that in this situation the protein obtains a new structure, α-helix, which is confirmed by the CD results. Thus, the interactions between the tail and the head do not diminish completely. According to conformation of subdomain A, that was reported by crystallographers, it has two extra disulfide bridges and two additional stable α-helices when compared to subdomain B [41]. The subpeaks of E1 and E2 relate to IIB and IIIB subdomains, respectively. Since both subdomains IIB and IIIB are placed at the tail part and both having nearly the same structure. However, IIIB has a specific site for glucose that increases its stability in a manner of T_m (see Table 1). The subpeak E4 is specified to IIIA and IB subdomains, because of the hydrophobic interactions between IIA and IIIA subdomains mediated by increased interactions with glucose. Here, the structural stabilization of IIIA is reduced (T_m is reduced to 334.5 K) that corresponds to the T_m of IB. Finally, E5 belongs to IA and IIA because of more compactness of the head part, IIA that contains Lys 199 (the second site of glucose binding) improving the stability of the head part. The increment of ΔH of unfolding in this case corresponds to the CD results that includes the presence of more helices.

The C_p^{excess} profile for interaction of HSA with glucose at 27.5 mM (Fig. 3) shows two portions of thermal denaturation than in Fig. 2. This implies that hydrophobic interactions between the tail and the head are disrupted at this glucose concentration. The co-operativity between the tail and the head decreases due to increasing concentration of glucose. Deconvolution of C_p^{excess} shows three subpeaks at the tail and one subpeak at the head. According to X-ray crystallography data, the DSC deconvoluted peak analysis shows three subpeaks (subdomains) for the tail and one for the head. The subpeaks of F1–F3 belong to IIB, IIIB and IIIA, respectively since at tail part IIIA has higher stability and IIIB is more stable than IIB due to binding of glucose at Lys 525. Finally, the F4 relates to the extra compacted head part of HSA in the presence of glucose that includes IA, IB and IIA subdomains. In this circumstance the hydrophobic relation between the head and the tail was separated completely.

In summary, our results show the hydrophobic interactions between IIA and IIIA subdomains that prepare the heart shape for HSA, having an effective role on stability of IIIA subdomain. Since this relationship diminishes considerable at 16.5 mM glucose concentration and disrupts at 27.5 mM glucose concentration, the T_m of IIIA reduces from about 338–325 K. Furthermore, this interaction prepares a suitable situation for creation of ligand binding sites at IIA subdomain. Thus, after glycosylation of HSA in diabetic patients the affinity of many ligands must be altered inevitably, especially the ligands that correspond to this site such as aspirin and long chain fattyacids. It is important to note that after glycosylation of HSA the affinity binding of long chain fattyacids is reduced considerably by one-twentieth [1] and for aspirin by half [19]. Although the binding sites (Lys 199) [1,15] are minimally occupied by glucose, it is the conformational changes that occur upon glycosylation which has the main impact. This is perhaps true for other HSA ligands and it is very important for diabetic patients that should be considered.

We can conclude that the conformational changes were occurred due to incubation of HSA in the presence of glucose at different concentrations. The decrement of secondary structure (α-helices) accompanying with lower stability were happened at low glucose concentration (8.25 mM) while the increment of α-helices concomitant with higher stability induced at higher glucose concentrations (16.5 and 27.5 mM). The interaction of HSA with glucose reduced the interrelationship of subdomains in the tail while the head becomes more compacted.

Acknowledgements

The authors would like to thank Dr. N.Sheibani and Dr. C.M. Sorenson, Department of Ophthalmology and Visual Scinces, University of Wisconsin, and

Dr. Seiied Vaghef Hosain for their valuable comments on the manuscript. Financial support provided by the Research Council of the University of Tehran, and Ministry of Health and Medical Services are gratefully appreciated. Also the authors thank to laboratories of analytical biochemistry of Blood Transfusion Organization of Iran and Research Center of Genetics for their kind assistance due to HSA preparation and additional purification test.

References

[1] N. Shaklai, R.L. Garlick, H.F. Bunn, J. Biol. Chem. 259 (1984) 3812–3817.
[2] D.C. Carter, J.X. Ho, Adv. Protein Chem. 45 (1994) 153–203.
[3] J. Figg, T.H. Rossing, V.J. Fencle, Lab. Med. 117 (1991) 453–467.
[4] T. Peters, Jr., in: F.W. Putnam (Ed.), The Plasma Proteins, 2nd Edition, Vol. 1, Academic Press, New York, 1975, pp. 133–181.
[5] T.A. Waldmann, in: V.M. Rosenoer, M. Oratz, M.A. Rothschild (Eds.), Albumin Structure, Function and Uses, Pergamon Press, Oxford, 1977, pp. 255–273.
[6] R. Dalhofer, O.H. Wieland, FEBS Lett. 103 (2) (1979) 282–286.
[7] U. Kragh-Hansen, Pharmacol. Rev. 33 (1) (1981) 17–53.
[8] J.R. Brown, P. Shockley, in: P.C. Jost, O.H. Griffith (Eds.), Lipid–Protein Interaction, Vol. 1, Wiley, New York, 1982, pp. 26–68.
[9] H.F. Bun, K.H. Gabbay, P.M. Gallop, Science 200 (1978) 21–27.
[10] E. Schleicher, T. Deufl, O.H. Wieland, FEBS Lett. 129 (1981) 1–4.
[11] M. Brownlee, A. Cerami, Ann. Rev. Biochem. 50 (1978) 385–432.
[12] J.W. Bayness, S.R. Thorp, M.H. Murtishaw, Methods Enzymol. 106 (1984) 88–98.
[13] A.J. Furth, Anal. Biochem. 175 (1984) 347–360.
[14] T. Arakawa, S.N. Timasheff, Biochemistry 21 (1982) 6536–6544.
[15] R.L. Garlick, J.S. Mazer, J. Biol. Chem. 258 (10) (1983) 6142–6146.
[16] A. Dugaiczyk, S.W. Law, O.E. Dennison, Proc. Natl. Acad. Sci. U.S.A. 79 (1982) 71–75.
[17] H.F. Bunn, R. Shapiro, M. McManus, L. Garlick, M.J. McDonald, P.M. Gallop, K.H. Gobbay, J. Biol. Chem. 254 (1979) 3892–3898.
[18] R. Shapiro, M.J. McManus, C. Zalut, H.F. Bunn, J. Biol. Chem. 255 (1980) 3120–3127.
[19] J.F. Day, S.R. Thorpe, J.W. Bayness, J. Biol. Chem. 254 (3) (1979) 595–597.
[20] S.R. Thorpe, J.W. Bayness, in: M.I. Horwitz (Ed.), The Glycoconjugates, Vol. 3, Academic Press, New York, 1982, p. 113.
[21] E. Schleicher, O.H. Wieland, J. Clin. Chem. Clin. Biochem. 19 (1981) 81–87.
[22] K.A. Mereish, H. Rosenberg, J. Cobby, J. Pharm. Sci. 71 (2) (1982) 235–238.
[23] M. Brownlee, A. Cerami, Annu. Rev. Biochem. 50 (1981) 385–432.
[24] J.D. Mcpherson, B.H. Shilton, D.J. Walton, Biochemistry 27 (1988) 1901–1907.
[25] K.M. West, Epidemiology of Diabetes and its Vascular Lesions, Elsevier, New York, 1987 (Chapter 6).
[26] M. Brownlee, H. Vlassara, A. Cerami, Annal. Int. Med. 101 (1984) 527–537.
[27] P.L. Privalov, Y.V. Griko, S.Y. Venyaminov, V.P. Kutyshenko, J. Mol. Biol. 190 (1986) 487–498.
[28] P.L. Privalov, S.A. Potekhin, Methods Enzymol. 131 (1986) 4–51.
[29] J. Sturtevant, Annu. Rev. Phys. Chem. 38 (1978) 463–488.
[30] H. Fukada, J. Sturtevant, F. Quiocho, J. Biol. Chem. 258 (1983) 13193–13198.
[31] B. Farruggia, J.A. Pico, Biochem. Biophys. Acta 1429 (1999) 299–306.
[32] J.A. Pico, Int. J. Biol. Macromol. 20 (1997) 63–73.
[33] J.M. Sanchez-ruiz, Biophys. J. 61 (1992) 921–935.
[34] P.L. Privalov, Adv. Protein Chem. 33 (1979) 167–241.
[35] P.L. Privalov, FEBS Lett. 40 (1973) S140–S153.
[36] K.P. Murphy, E. Freier, Adv. Protein Chem. 43 (1992) 313–361.
[37] K.S. Krishnan, J.F. Brandts, Methods Enzymol. 49 (1978) 3–14.
[38] J.M. Sanchez-ruiz, in: B.B. Biswas, Siddhartha Roy (Eds.), Subcellular Biochemistry, Proteins: Structure, Function, and Engineering, Vol. 24, Plenum Press, New York, 1995, pp. 133–176.
[39] R.L. Baldwin, Proc. Natl. Acad. Sci. 83 (1986) 8069.
[40] D.C. Carter, X.M. He, S.H. Munson, P.D. Twigg, K.M. Gernert, M.B. Broom, T.Y. Miller, Science 244 (1989) 1117–1122.
[41] X.M. He, D.C. Carter, Nature 358 (1992) 209–215.